SUPPLEMENTARY INFORMATION

Exploring Controls on the Fate of PVP-Capped Silver Nanoparticles in Primary Wastewater Treatment

Stephen M. King[a], Helen P. Jarvie, Michael J. Bowes,
Emma Gozzard, Alan J. Lawlor and M. Jayne Lawrence

ISIS Facility, STFC Rutherford Appleton Laboratory, Harwell Oxford
Didcot, OX11 0QX, United Kingdom, [a]*Corresponding author,*
Tel: +44 (0)1235 446437; e-mail: *stephen.king@stfc.ac.uk*

Table S1 Purity of the silver nanopowder *(manufacturers data)*

Manufacturer:	American Elements (Merelex Corporation)
Product Code:	AG-M-025M-NPC.030N

| Element	Impurity Concentration (ppm)
Al	82
As	3
Bi	51
Cu	72
Fe	91
Ni	53
Si	23

The nanopowder is partially passivated with oxygen (to give a ~2 nm thick oxide layer) for safe shipping and handling, and coated with ~0.2 %$^w/_w$ poly(vinylpyrolidone), PVP, $(C_6H_9NO)_n$, stabiliser for easy dispersion. The molecular weight of the PVP is ~6000 g/mol (i.e., n~54).

Table S2 TEM particle size analysis of the silver nanopowder *(manufacturers data)*

| Diameter (nm)	Number Fraction (%)	Cumulative Total (%)
1 - 5	4.1	4.1
5 - 10	11.3	15.4
10 - 18	37.6	53.0
18 - 36	23.7	76.7
36 - 60	6.1	82.8
60 - 96	5.3	88.1
96 - 140	3.3	91.4
140 - 200	3.2	94.6
200 - 300	5.4	100.0

Thus 61 % of the particles have a median diameter of ~23 ± 13 nm; i.e. median radius of 11.5 ± 6.5 nm (11.5 ± 56 %). The average particle size (APS) quoted by the manufacturer is 20 – 30 nm.

Figure S1 Comparison of particle size distributions
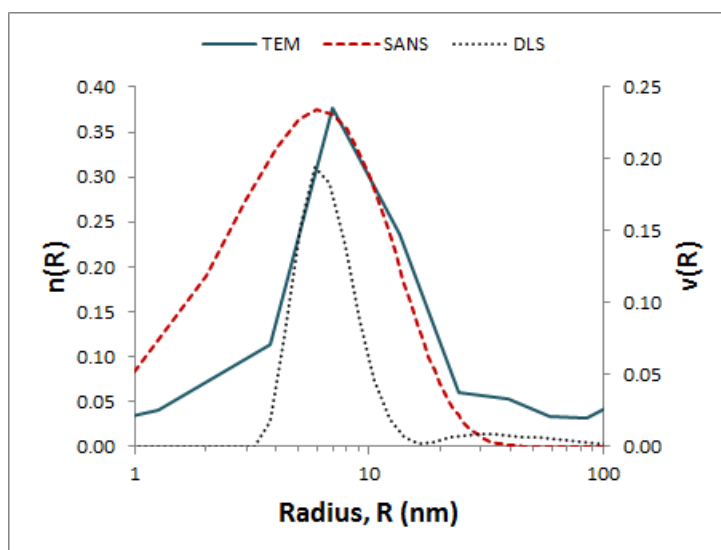
Graph comparing the manufacturers TEM particle size distribution data (see Table S2) with that derived from both DLS and the best model-fits to the SANS data using different aqueous dispersions but of the same nanoparticles and measured as part of the present work. The form of the SANS size distribution is described by a Schultz polydispersity function (<R> = 11.5 nm, σ/<R> = 0.6), see *Analysis of small-angle neutron scattering spectra from polydisperse interacting colloids*. M. Kotlarchyk, S.-H. Chen. *J. Chem. Phys*. 1983, 79, 2461-2469. The SANS distribution has been rescaled to match the peak number fraction in the TEM distribution. The DLS data are expressed as particle volume fraction and were measured on a Malvern Zetasizer (~1 mg/ml dispersion in water; n_{Ag} = 0.2).

Figure S2 TEMs of the silver nanopowder *(present work)*


(a)   (b)   (c)   (d)
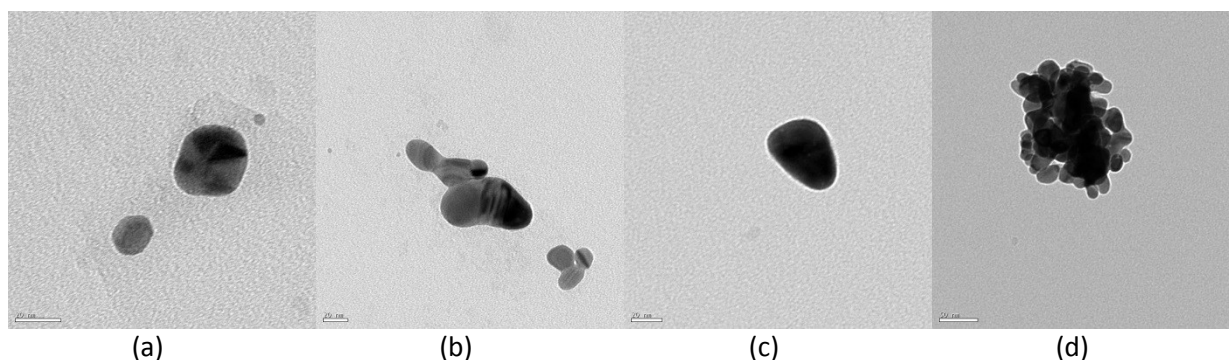
Transmission electron micrographs of American Elements silver nanopowder AG-M-025M-NPC.030N after dispersal in nanopure water. The scale bar (in the bottom left corner) is 20 nm in images (a) – (c), but 50 nm in image (d). The nanoparticles were deposited by spreading one or two drops of diluted aqueous AgNP dispersion on carbon-coated 200-mesh copper grids (TAAB Laboratories Equipment Ltd, UK) and allowing the water to evaporate. The images were recorded on a Philips Tecnai T20 microscope operating at 200 kV.

Figure S3 Picture of a silver nanopowder dispersion

The image shows a dispersion of American Elements silver nanopowder AG-M-025M-NPC.030N in nanopure water at a concentration of 0.19 %^{v}/$_v$, equivalent to ~2 %^{w}/$_w$. The pathlength of the cuvette shown, used for some preliminary SANS measurements, is 2 mm.

Figure S4 Estimation of the radius-of-gyration of the PVP stabiliser
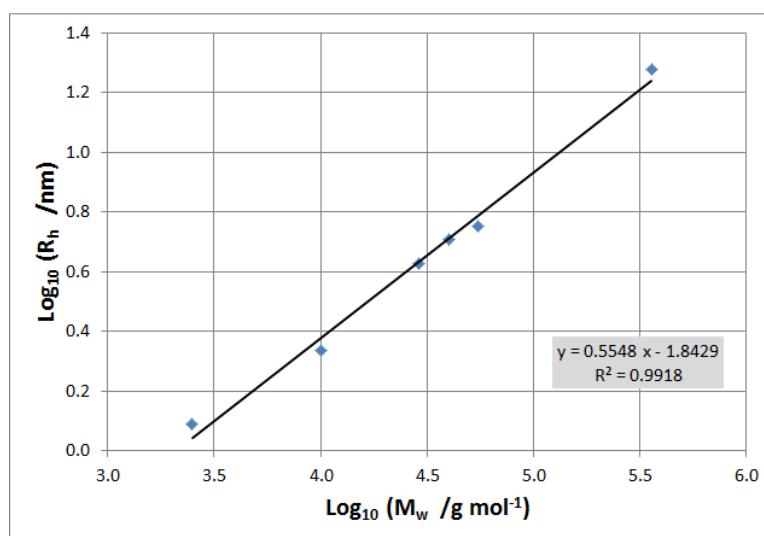
The PVP data plotted above are taken from *The Hydrodynamic Radii of Macromolecules and Their Effect on Red Blood Cell Aggregation*. J. K. Armstrong, R. B. Wenby, H. J. Meiselman, and T. C. Fisher, *Biophys J*. Dec 2004, 87(6), 4259–4270. doi: 10.1529/biophysj.104.047746.

R_h is the effective hydrodynamic radius of a sphere having the same viscometric behaviour as the polymer coil. The equivalent radius-of-gyration $R_g = (3/5)^{1/2} R_h$. For M_w= 6000, the value for the stabiliser quoted by the silver nanopowder manufacturer, R_g = 1.4 nm.

Figure S5 Schematic representation of a silver nanoparticle
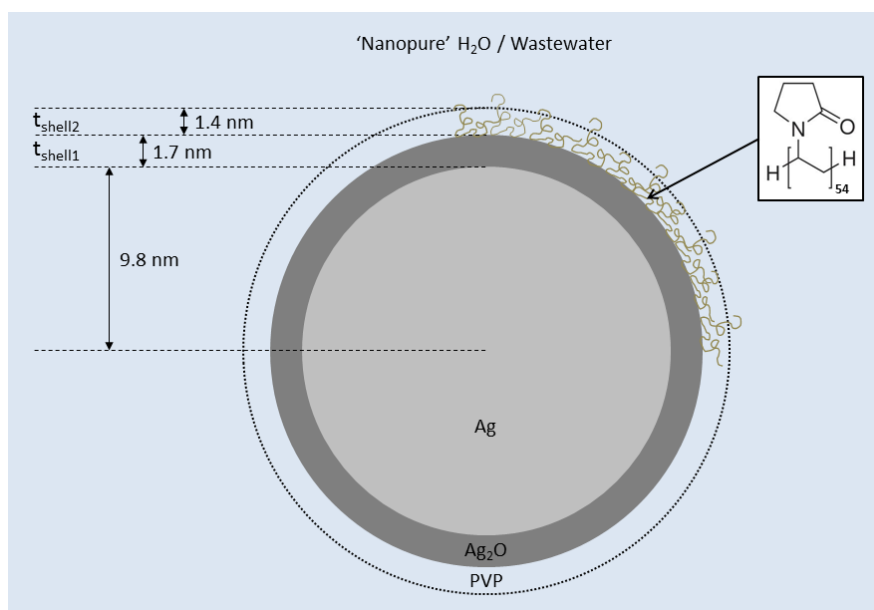
The image shows a schematic cross-section through a silver nanoparticle based on a synthesis of all the available characterisation data. Though a spherical morphology is depicted, and indeed to a first approximation is a reasonable description, the actual nanoparticles are not perfectly spherical and also exhibit significant size polydispersity. The PVP layer should be considered free-draining.

Table S3 Neutron scattering length densities and contrasts

The neutron *scattering length density* (NSLD) ρ of a molecule is given by:

$$\rho = \frac{\delta \cdot N_A \cdot \sum_{i=1}^{n} b_i}{M} \qquad \text{(SI-1)}$$

where δ is the macroscopic bulk density of the molecule, M is its molecular weight, b_i is the coherent nuclear scattering length of atom i, and the summation extends over all atoms in the molecule. Values of b for the various elements may be found in standard tables or on the world-wide web. Data analysis programs such as SasView (http://www.sasview.org/) include a NSLD calculator tool.

The neutron scattering *contrast* of a molecule is the difference in NSLD between that molecule and another, usually the matrix. The NSLD of the composite nanoparticle is calculated as a *volume-weighted* linear combination of the NSLDs for Ag, Ag$_2$O and PVP (also see Figure S5).

Material	Fraction of NP Volume (%)	NSLD, ρ (/10^{10} cm^{-2})	Contrast, ρ -ρ_{H2O} (/10^{10} cm^{-2})
H$_2$O	-	-0.56	0.00
PVP	29.2	+1.39	1.95
Ag$_2$O	27.0	+3.27	3.83
Ag	43.9	+3.47	4.03
Composite AgNP	100.0	+2.81	3.37

Figure S6 Model fits to the SANS data from the nanoparticle dispersion in nanopure water
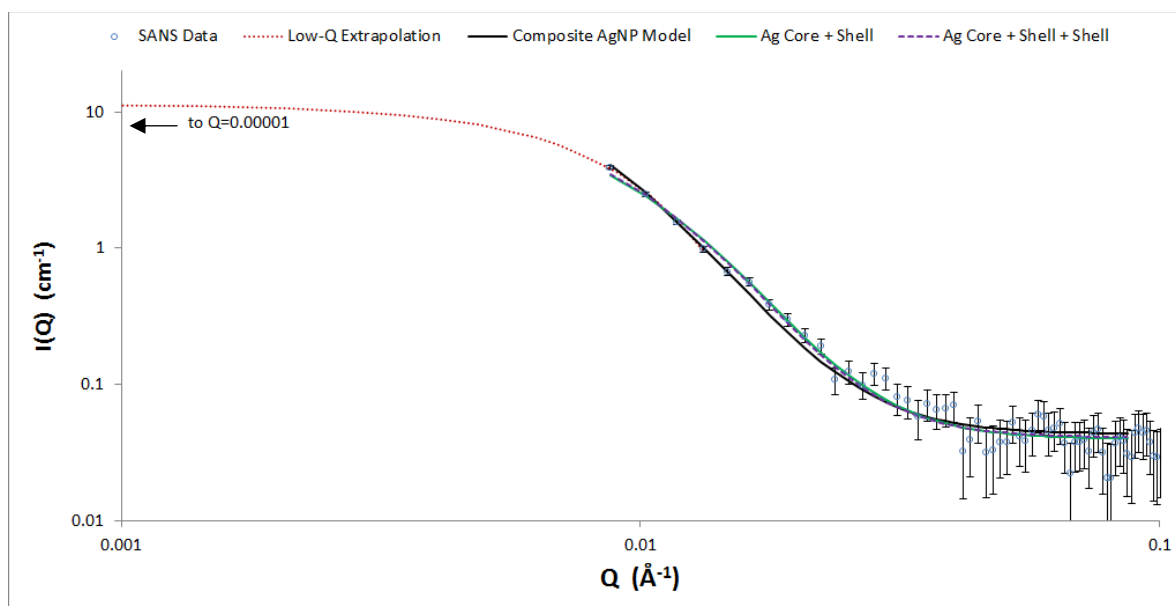
The SANS data shown above is from a 1.6 $\%^w/_w$ (0.15 $\%^v/_v$) stock dispersion of the silver nanoparticles in nanopure water.

Table S4 SANS characterisation of the nanoparticle dispersion in nanopure water

Model:	Composite AgNP	Ag Core + Shell$_1$	Ag Core + Shell$_1$ + Shell$_2$
Q-range fitted (Å^{-1})	0.00875 – 0.0875	0.00875 – 0.0875	0.00875 – 0.0875
ρ_{matrix} (/10^{10} cm^{-2})	-0.56	-0.56	-0.56
$\rho_{particle}$ (/10^{10} cm^{-2})	+2.81	+3.47	+3.47
ρ_{shell1} (/10^{10} cm^{-2})	-	+3.27	+3.27
ρ_{shell2} (/10^{10} cm^{-2})	-	-	+1.39
Contrast (/10^{10} cm^{-2})	3.37	4.03	3.95
$R_{particles}$ (nm)	12.9	9.8	9.8
$\sigma/<R_{particles}>$	0.56	0.56	0.56
t_{shell1} (nm)	-	1.7	1.7
σ/t_{shell1}	-	0.10	0.10
t_{shell2} (nm)	-	-	1.4
σ/t_{shell2}	-	-	0.1
Porod Invariant (cm^{-1}Å^{-4})	3.89×10^{-5}	3.89×10^{-5}	3.89×10^{-5}
$\chi^2/N_{datapoints}$	0.968	1.061	0.994
Background (cm^{-1})	0.043	0.039	0.041
$\phi^0_{particles,fit}$ (from fit)	0.00022	0.00015	0.00017
$\phi^0_{particles,invariant}$ **(using P.I.)**	**0.0017**	**0.0012**	**0.0012**
$\phi^0_{particles,actual}$ **(actual dosed)**	**0.0015**	**0.0015**	**0.0015**

The table shows the best parameters obtained from least-squares fits to three different models of the silver nanoparticles (refer to Figure S5): 'Composite AgNP' = a homogeneous sphere of a volume-average NSLD and overall radius *including* the Ag$_2$O and PVP shells; 'Ag core + shell$_1$' = a model

specifically accounting for the Ag core and Ag_2O shell of the NP *but not* the PVP shell; 'Ag core + $shell_1$ + $shell_2$' = a model specifically accounting for the Ag core, the Ag_2O shell *and* the PVP shell of the NP. The grey shading indicates those parameters that were fixed. Only the incoherent background and apparent particle volume fraction, $\phi_{particles}$, were allowed to vary during the fitting. Bold type denotes the final adjusted particle volume fraction derived from the SANS data and, for comparison, the known particle volume fraction on dosing.

As can be seen from the table, and from Figure S6 above, all three particle models are good descriptions of the SANS data, but the 'Composite AgNP' model is more than capable of reproducing the nanoparticle concentration without the additional complexity of the other models.

Note: As the measurement range of the LOQ SANS instrument did not extend far enough into the higher end of the particle size distribution ($2\pi/Q_{min}$ ~ 70 nm) not all of the scattering curve was recorded and this has led the model-fits to report an apparent under-estimation of the particle volume fraction (by about a factor 10 in this instance). Fortunately, because the nanoparticles are discrete and approximately spherical, it is possible to recover this missing information through Guinier extrapolation of the SANS data to lower Q values (here to Q = 0.00001 Å^{-1}) and calculation of a quantity known as the (Porod) Invariant (or Total Scattering). The Invariant (see below) depends only on the scattering contrast and the volume fraction of material present; it will be a constant for a given sample. Thus it can be used to recover the true experimental particle volume fraction which can, in turn, be used to rescale that derived from the model fits. When this is done all three models are seen to return the same volume fraction for any chosen contrast. In the case of the 'Composite AgNP' model the experimentally-determined particle volume fraction is found to be within about 13% of the known concentration on dosing (and ignoring settling/sedimentation during the reference SANS measurement), proof that the model and rescaling procedure are quite robust. The proportion of the Invariant contributed by the extrapolated region below Q~0.01 Å^{-1} is <4 % of the total.

The Porod Invariant

For an incompressible, two-phase, system such as the nanoparticle dispersion, the Porod Invariant (or Total Scattering) is given by (G. Porod, *Kolloid Z.* 1952, 125, 51-57):

$$P.I. = \int_0^\infty Q^2 \, I(Q) \, dQ = 2 \pi^2 \, \phi_{particles}(1 - \phi_{particles}) \, (\rho_{particle} - \rho_{medium})^2$$

The only difficulty in using this construct is in ensuring that the integral is closed, and this is where low-Q, and sometimes high-Q, extrapolations are necessary. In this work the integral was taken over the range from Q = 0.00001 (by extrapolation) to the maximum Q of the data.

Volume fraction correction

Having obtained a good 'Composite AgNP' model fit to data from a dispersion of just the AgNP in nanopure water measured for an extended duration, and subsequently derived the corresponding values of $\phi_{particles,fit}$, $\phi_{particles,invariant}$, and R (each denoted by the superscript '0' below), the volume fraction of particles returned by model fits to all other datasets were then corrected according to

$$\phi_{particles,fit,corrected} = \phi_{particles,invariant}^0 \times \left(\frac{\phi_{particles,fit}}{\phi_{particles,fit}^0} \right) \times \left(\frac{R_{fit}}{R_{fit}^0} \right)^3$$

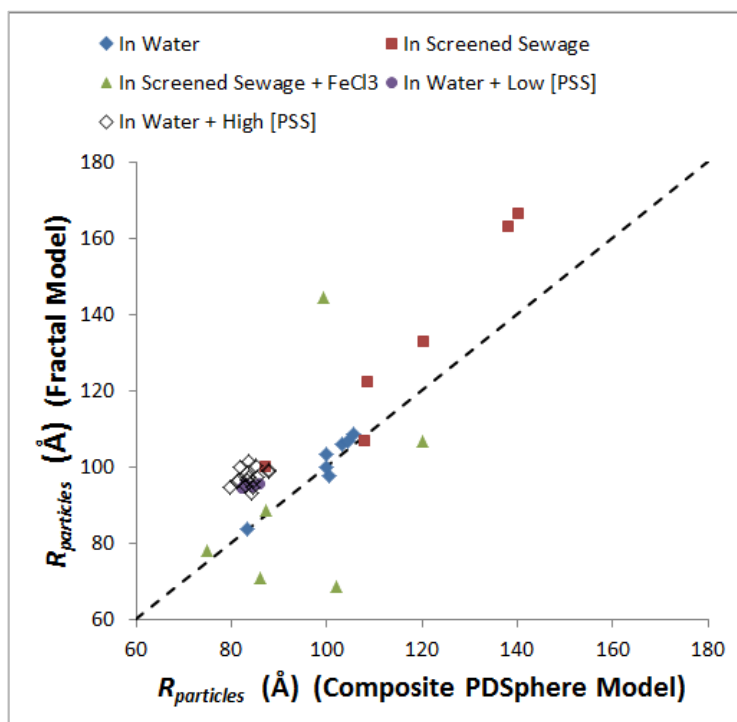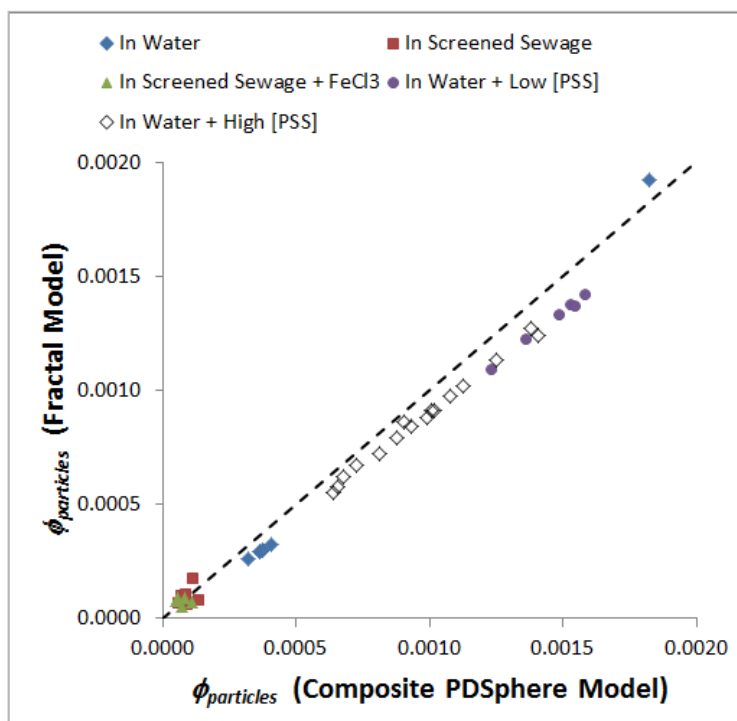**Figure S7(a)** Correlations in derived particle radius

Figure S7(b) Correlations in derived particle volume fraction

Graphs showing the correlations in derived particle size (radius) and particle concentration (volume fraction) between the Composite Polydisperse Spheres Model and the Fractal Model.

Table S5 Wastewater treatment plant and wastewater characteristics

Raw (untreated) wastewater was sourced from the inlet stream (immediately after screening and grit removal) of a Wastewater Treatment Plant in South Oxfordshire, England, serving a rural population of 6,230 people. The WWTP receives flow from a number of pumping stations, either running in series to the site along the sewer network, or in parallel from sub-catchments. The consented dry weather flow (DWF) to works is 2,517 m^3 day^{-1}, however the average annual DWF is 1,368 m^3 day^{-1}. The WWTP has both primary and secondary sedimentation steps (with a hydraulic retention time of 7 – 8 hours at DWF) and trickling filters as the main biological treatment step.

Wastewater sample collection performed on Monday 3rd May 2010 at 10:15 GMT	
Water temperature (°C)	12.2
pH	7.87
Conductivity (μS/cm)	1079
Total Dissolved Solids (ppm)	763.8
SRP (μg/L-P)	3990
TDP (μg/L-P)	4380
TP (μg/L-P)	5260
NH_4 (mg/L)	4200
Cl (mg/L)	91.5
NO_2 (mg/L)	3.25
Br (mg/L)	0.062
NO_3 (mg/L)	20.2
SO_4 (mg/L)	61.0
TDN (mg/L)	7.82

Wastewater sample collection performed on Tuesday 18th November 2014 at 09:40 GMT	
pH	7.39
Conductivity (μS/cm)	1092
Total Suspended Solids (mg/L)	259.6

Wastewater sample collection performed on Monday 1st December 2014 at 10:03 GMT	
pH	8.11
Conductivity (μS/cm)	1122

Table S6 Results of the bench-top settling experiments in wastewater (2014)

| Sample	Time (hr)	Measuring Position	Distance settled [a,b] (mm)	[Ag] (μg/L)	Loss/(gain) (%)	v_s (mm/hr)
t=0	0.03	Top		679.6		
t=15	0.28	Top	94.5	383.3	44	163
t=45	0.82	Top	90.7	312.8	54	73
t=120	2.10	Top	90.7	255.6	62	33
t=15	0.30	Bottom	661.5	n/a [c]		
t=45	0.83	Bottom	635.2	269.2		
t=120	2.12	Bottom	635.2	319.8	(19) [d]	

[a] One of the burettes was a different diameter to the other two. [b] Distance given is to *mid-point* of the volume sampled. [c] A valid sample could not be recovered in time due to a blockage in the burette tip. [d] Minimum value using the t=45 sample instead of the t=15 sample.

Figure S8 Effect of FeCl$_3$ flocculant on the SANS from screened wastewater only
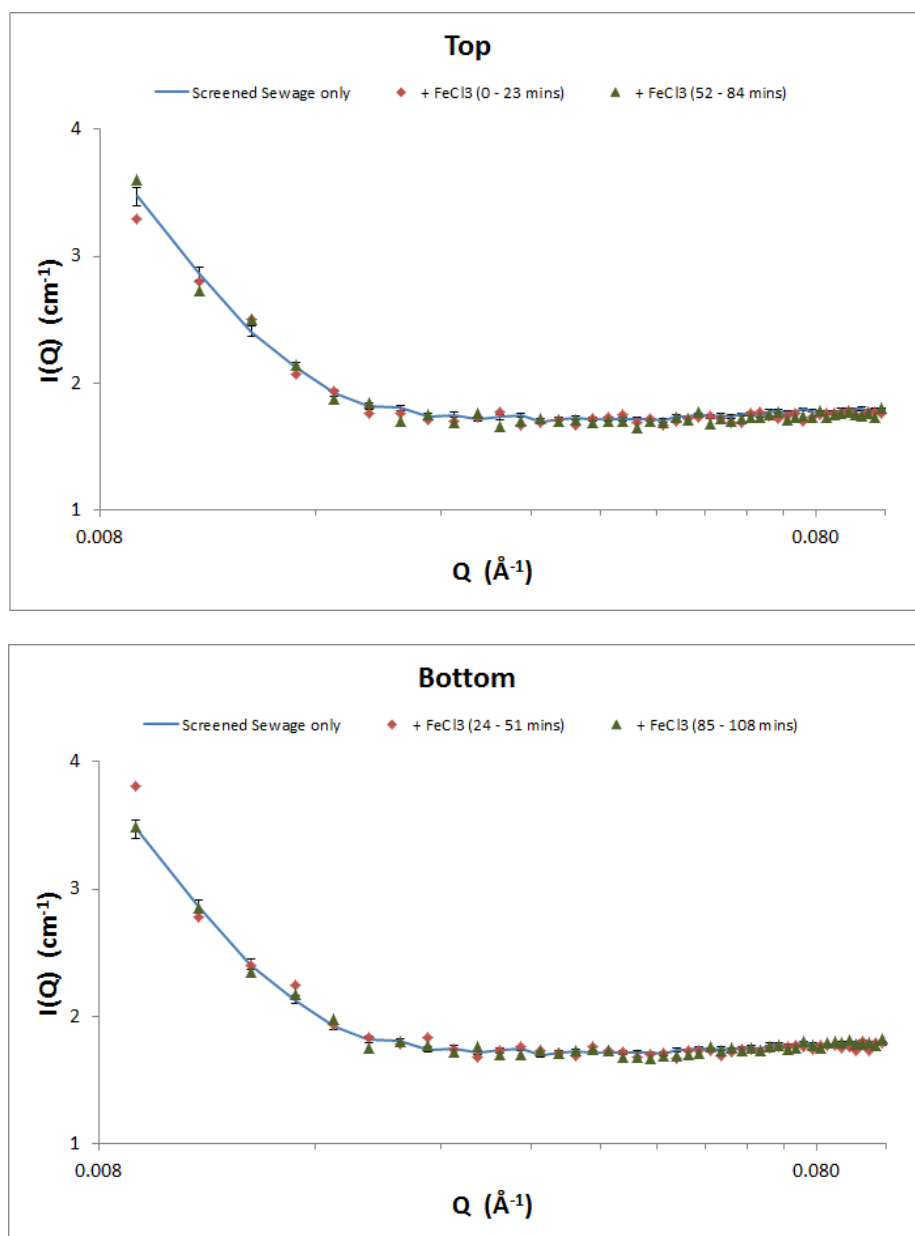
Graphs showing that dosing just screened sewage (no nanoparticles) with 30 mg/L FeCl$_3$ flocculant has no effect on the measured SANS signal even after 1.5 hours. Note that the background scattering from the sample cuvettes has not been subtracted from these data.

Figure S9a Impact of particle volume fraction on the colloidal structure factor and SANS
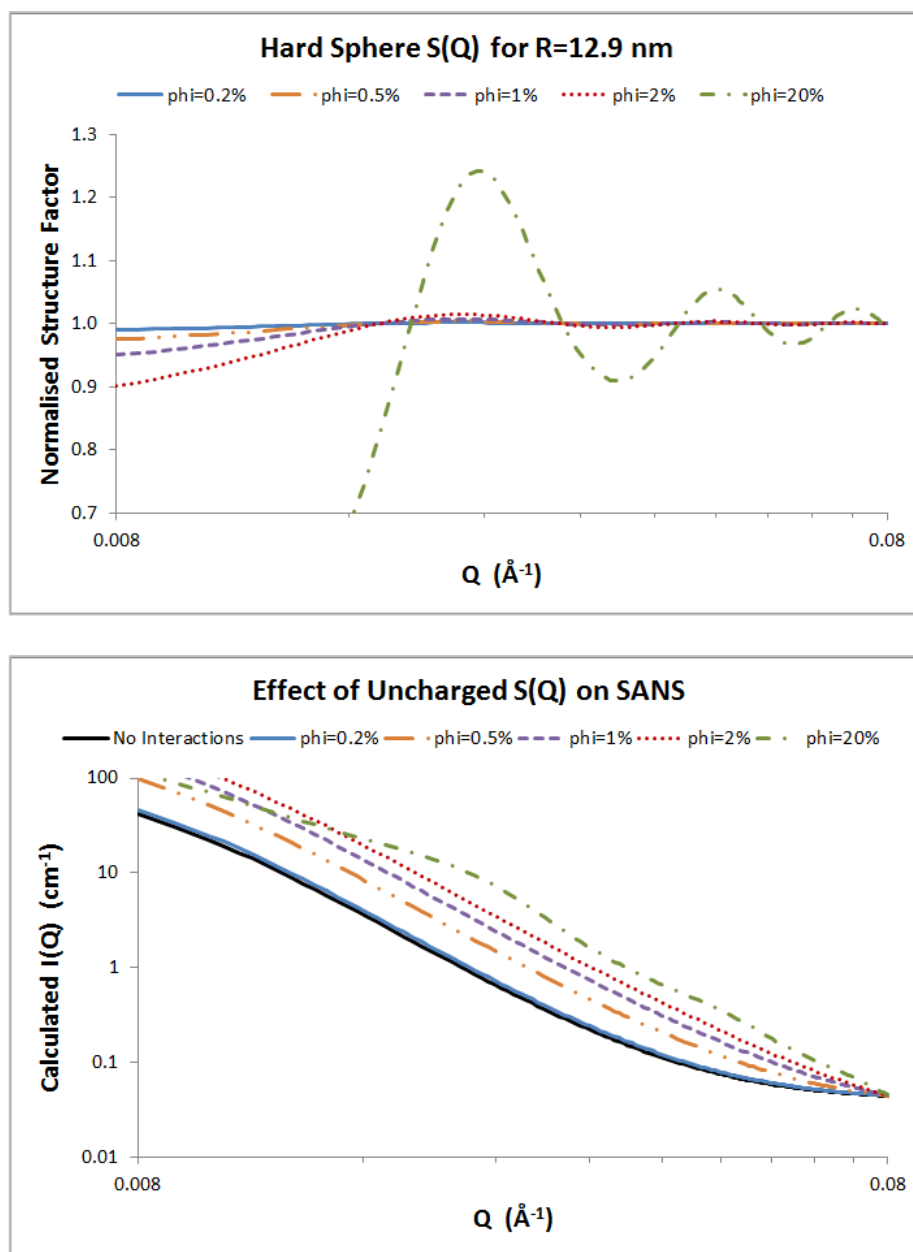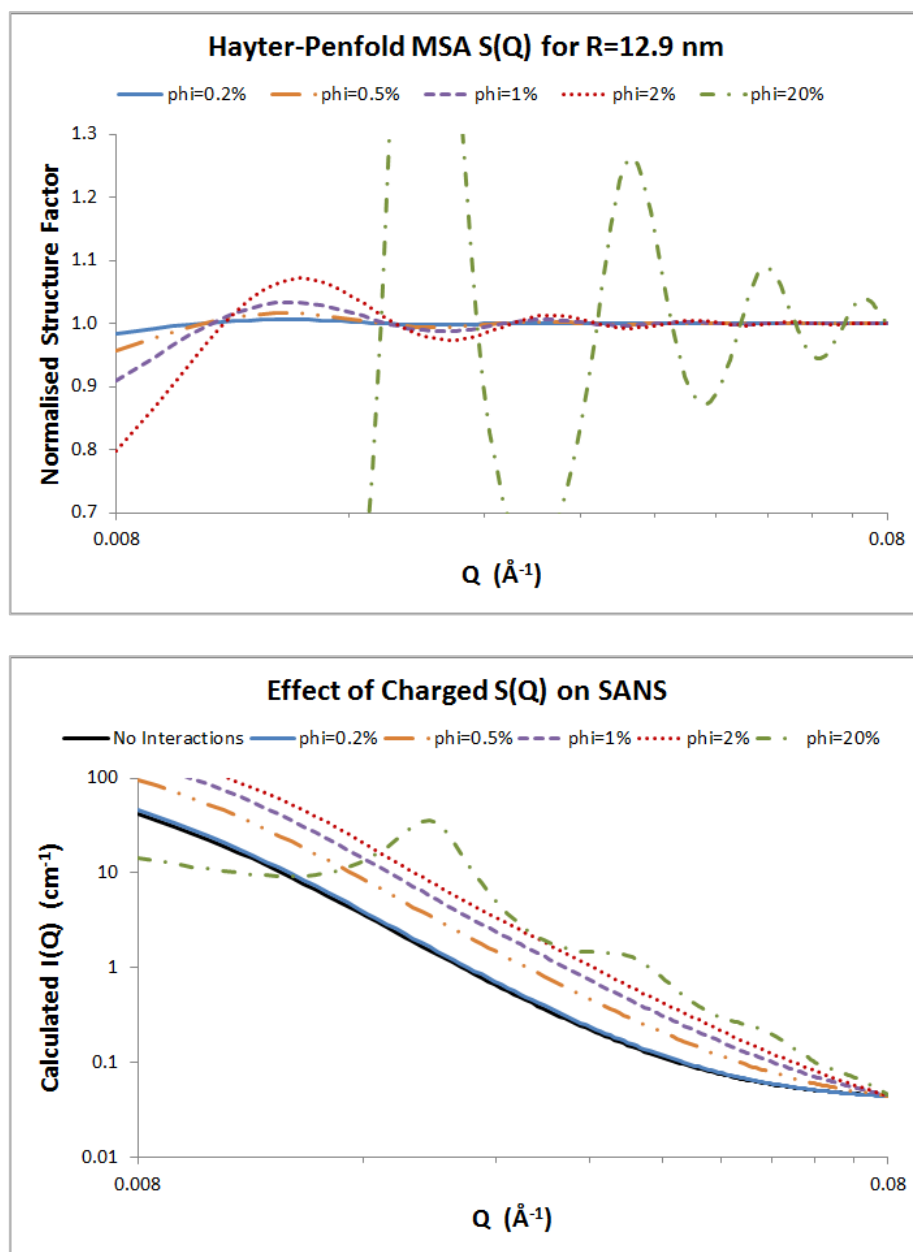

Calculations of the colloidal structure factors, and their impact on the SANS, for polydisperse spherical particles of $R_{particles}$ = 12.9 nm and $\sigma/R_{particles}$ = 0.56 (see Figure S5 and Table S4) at particle volume fractions, $\phi^0_{particles}$, of 0.2, 0.5, 1.0, 2.0 and 20%. The 'no interactions' reference scattering (black line) is intended to approximate the fit in Figure 1, bottom-left pane.

These graphs incorporate a simple hard-sphere (excluded volume) pair potential with Percus-Yervick closure and represent the case of *uncharged* particles (see *Analysis of Classical Statistical Mechanics by Means of Collective Coordinates*. J. K. Percus and J. Yervick, *Phys. Rev.* 1958, 110, 1).

As can be seen, at the particle volume fraction used in this work, $\phi^0_{particles}$ = 0.19%, particle-particle interactions are negligible.

Figure S9b Impact of particle volume fraction on the colloidal structure factor and SANS


Calculations of the colloidal structure factors, and their impact on the SANS, for polydisperse spherical particles of $R_{particles}$ = 12.9 nm and $\sigma/R_{particles}$ = 0.56 (see Figure S5 and Table S4) at particle volume fractions, $\phi^0_{particles}$, of 0.2, 0.5, 1.0, 2.0 and 20%. The 'no interactions' reference scattering (black line) is intended to approximate the fit in Figure 1, bottom-left pane.

These graphs use the Hayter-Penfold Mean Spherical Approximation for screened Coulomb repulsion between *charged* particles in a dielectric medium: assuming 295 K, in water, with 0.01 M monovalent salt, and a particle charge of 500 e; ie, highly charged particles (see *An Analytic Structure Factor for Macroion Solutions*. J. H. Hayter and J. Penfold, *Mol. Phys.* 1981, <u>42</u>, 109).

As can be seen, at the particle volume fraction used in this work, $\phi^0_{particles}$ = 0.19%, particle-particle interactions are negligible.

Figure S10 Resilience of the AgNPs to dissolution in different matricies
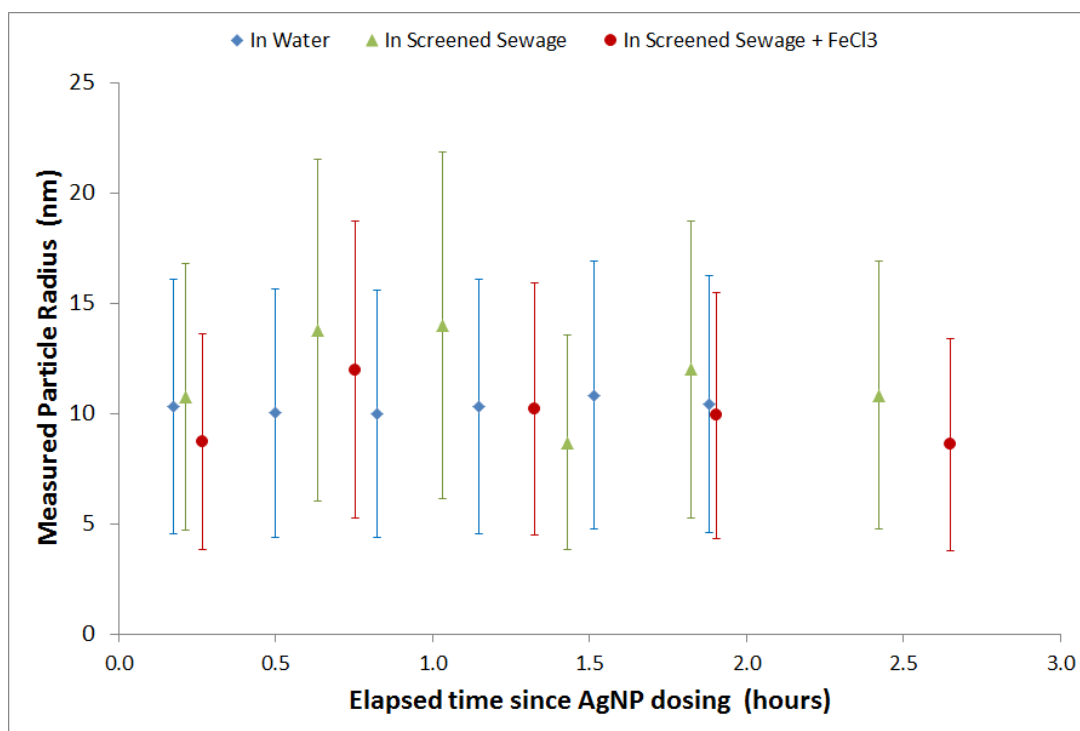
Graph of the measured particle size (as derived from the SANS model-fitting) as a function of time. The error bars shown represent the known width of the particle size distribution. There does not appear to be any significant dissolution of the AgNPs on the timescales of the measurements.

Figure S11 Rate of change of the experimentally-derived settling velocity
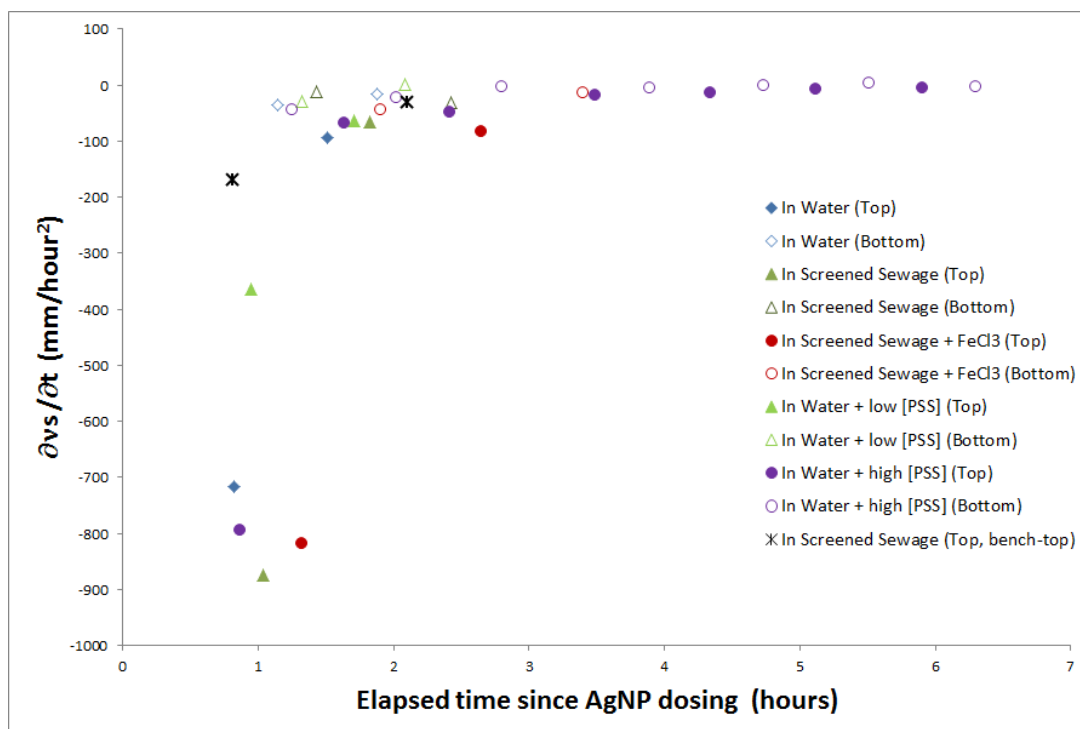
Figure S12 Temperature history at the LOQ sample position during the SANS experiments